JMEPEG (2012) 21:854–858
DOI: 10.1007/s11665-011-9952-x

©ASM International
1059-9495/$19.00

Resistivity Distribution of Multicrystalline Silicon Ingot Grown by Directional Solidification

S.H. Sun, Y. Tan, W. Dong, H.X. Zhang, and J.S. Zhang

(Submitted May 3, 2010; in revised form April 10, 2011)

The effects of impurities on the resistivity distribution and polarity of multicrystalline silicon ingot prepared by directional solidification were investigated in this article. The shape of the equivalence line of the resistivity in the vertical and cross sections was determined by the solid-liquid interface. Along the solidification height of silicon ingot, the conductive type changed from p-type in the lower part of the silicon ingot to n-type in the upper part of the silicon ingot. The resistivity in the vertical section of the silicon ingot initially increased along the height of the solidified part, and reached its maximum at the polarity transition position, then decreased rapidly along the height of solidified part and approached zero on the top of the ingot because of the accumulation of impurities. The variation of resistivity in the vertical section of the ingot has been proven to be deeply relevant to the distribution of Al, B, and P in the growth direction of solidification.

Keywords directional solidification, resistivity, silicon, solid-liquid interface

1. Introduction

With the rapid development of the photovoltaic industry, solar grade silicon (SoG-Si) feedstock has been in scarcity in recent years. Developing metallurgical refining process to purify abundantly available metallurgical grade silicon (MG-Si) to the preferred degree of purity has attracted a lot of concern among the researchers (Ref 1-7).

For SoG-Si, the preferred resistivity is needed to be within the range of 0.005-0.015 Ω m. The complexity of the impurity composition existing in MG-Si makes it difficult to control of the resistivity of the multicrystalline silicon refined by MG-Si. The resistivity distribution in the multicrystalline silicon ingot prepared by directional solidification process with the feedstock containing 0.2-10 ppma boron and 0.1-10 ppma phosphorous has been given in a US patent (Ref 8). The cited previous study indicated that the resistivity of the ingot was described by an exponential curve having a starting value between 0.004 and 0.1 Ω m, with the resistivity increasing toward the top of the ingot where the p-n type transition occurred. However, the effect of impurities on the resistivity of silicon ingot was not discussed in detail. Considering only boron and phosphorus as the donor and acceptor concentrations respectively, and considering their segregation and the effect of compensation on the carriers, Dhamrin et al. (Ref 9) provided a simple calculation technique to determine the resistivity distribution in the directional solidification ingot. However, as the complexity of impurity composition existed in MG-Si, the resistivity distribution of multicrystalline silicon ingot prepared by the MG-Si is difficult to be determined with only B and P being considered.

In this article, the effect of impurities on the resistivity distribution and polarity of multicrystalline silicon prepared by MG-Si were investigated.

2. Experimental

The schematic diagram of directional solidification assembly is shown in Fig. 1. It consists of a vacuum system, an induction heating system, and a pulling system. Graphite and quartz crucibles were used in the experiment. Three thermocouples named T1, T2, and T3 for temperature control were placed just next to the quartz crucible with an interval of 0.050 m vertically along the quartz crucible. The experiment showed that error of the temperature T' measured in the inner silicon and the temperature T measured on the side of the quartz crucible could be expressed as $(T' - T)/T' < 0.5\%$, so that T can be used to indicate T'. The composition of the MG-Si used in this experiment is shown in Table 1. 7 kg of MG-Si was washed by deionized water and dried at 150 °C for 2 h, and then, it was loaded in a quartz crucible with the size of 0.190 m in diameter and 0.153 m in height. The inside of the furnace was evacuated to 0.1 Pa by a rotary pump and a roots pump, and the crucible was heated up to 1753 K as measured by T1. The temperature was then kept constant for 2 h to ensure that the feedstock got completely molten. The vacuum pump was then closed and back-filled with pure grade Ar gas (99.999%) until the pressure reached a value of 5.5×10^4 Pa. The temperature measured by T1 was decreased from 1753 to 1693 K by adjusting the power. The crucible was pulled out

S.H. Sun, Y. Tan, W. Dong, H.X. Zhang, and **J.S. Zhang**, School of Materials Science and Engineering, Dalian University of Technology, Linggong Road 2, Dalian 116024, China; **S.H. Sun, Y. Tan, W. Dong,** and **H.X. Zhang**, Key Laboratory for Solar Energy Photovoltaic System of Liaoning Province, Linggong Road 2, Dalian 116024, China. Contact e-mails: shihai528@yahoo.com.cn and w-dong@dlut.edu.cn.

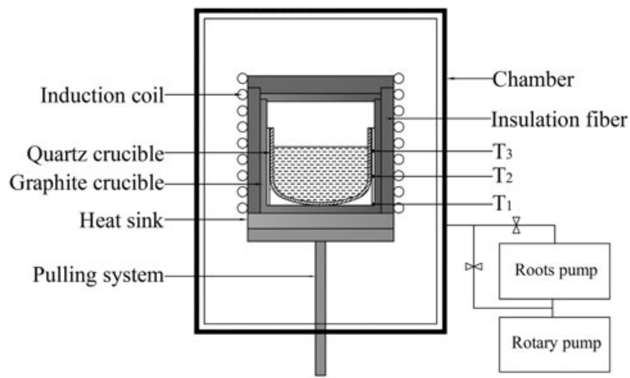

Fig. 1 Schematic of the experiment equipment

Table 1 Primary concentration of impurities in silicon feedstock (mass/×10^{-6})

Element	Fe	Al	Ca	Ti	Cu	Ni	Mn	B	P
Concentration	1384	140.4	31	86	9.4	28.7	20	2.3	33

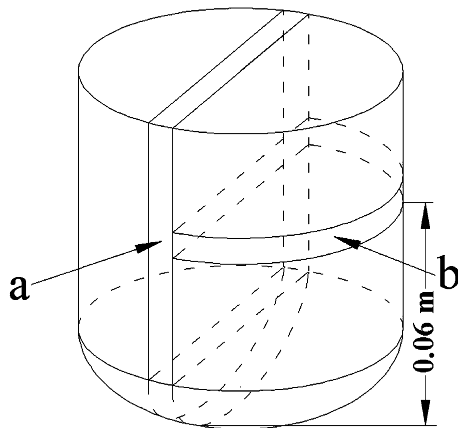

Fig. 2 Schematic of the sampling position

from the induction coil at a speed of 2×10^{-6} m/s. A vertical temperature gradient in the molten silicon was formed and the molten silicon began to solidify in the desired growth direction. After the molten silicon had solidified completely, the temperature was gradually lowered to 1273 K, and then the power was shut off.

To investigate the resistivity variation along the vertical and cross section of the silicon ingot, the obtained ingot was cut as shown in Fig. 2. To ensure the accuracy of the measured resistivity, the possible organic contamination and impurities from the surface were removed by etching the samples with 20 wt.% KOH. The conductive type of the vertical section was obtained using a polarity tester. In order to characterize the resistivity variation in different positions, the vertical and cross sections were divided into 1×10^{-4} m^2 grids, with the average resistivity of each grid tested by four-point resistivity test system (KDY-1). Meanwhile, in order to investigate the relationship between the resistivity and the impurities, seven samples were taken from the bottom to the top along the

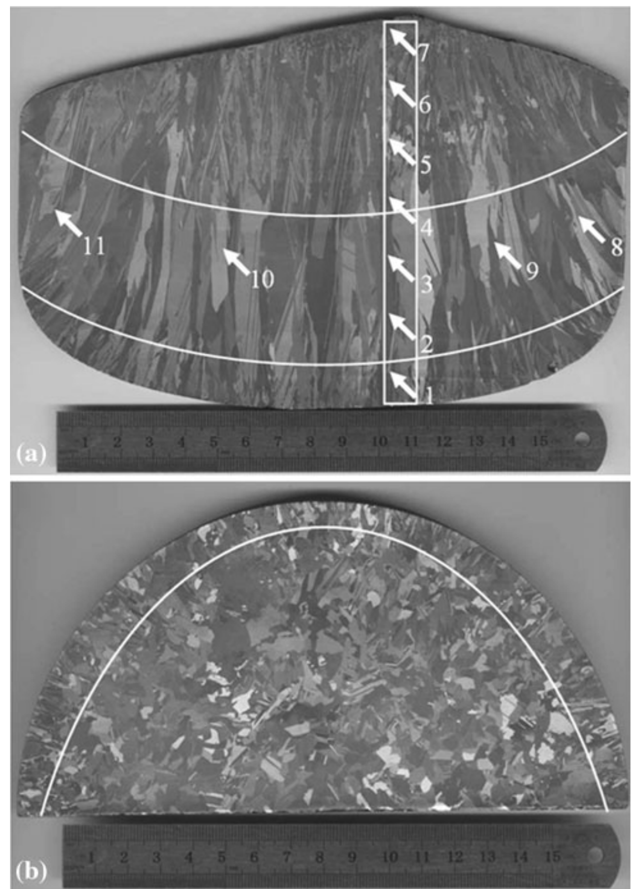

Fig. 3 Macrostructure of the silicon: (a) macrostructure of the vertical section of the silicon ingot, and (b) macrostructure of the cross section of the silicon ingot

vertical section, with a little deviation from the geometric center axial, and five samples were taken on different parts of the 3.3×10^{-3} Ω m resistivity equivalence line, as shown in Fig. 3. The concentration of impurities was analyzed by ICP-AES (Optima 2000DV).

3. Results and Discussion

3.1 Resistivity Distribution of the Multicrystalline Silicon

The obtained silicon ingot was 0.13 m in height, and 6.6 kg in weight. The surface was convex and a tip-like protuberance existed in the center part, a result of the density of liquid being larger than that of solid silicon. The macro-structure of the silicon is shown in Fig. 3. Three different microstructures existed in the ingot as shown in Fig. 3(a), with small columnar grains at the bottom, large columnar grains at the central part, and dendritic grains at the top. The position of the breakdown area existing between the large columnar grains and dendritic grains was 0.07 m from the bottom in the central part (54% of the height). The grain growth direction in the central area was along the axial, whereas it was a slightly tilted in the other area. Because the grain growth direction was perpendicular to the solid-liquid interface, the curvatures shown in Fig. 3(a) represented the solid-liquid interface shape in different growth steps.

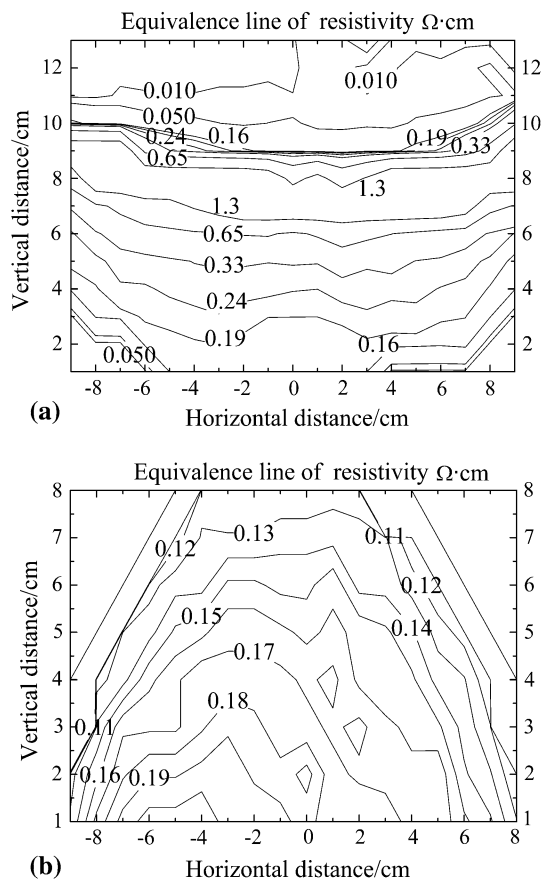

Fig. 4 Resistivity distribution of the silicon ingot: (a) resistivity distribution in the vertical section of the silicon ingot, and (b) resistivity distribution in the cross section of the silicon ingot

As shown in Fig. 3(b), there existed two different microstructures, equiaxed grains in the inner area and small slender-shaped grains toward to the radial direction on the side, which was caused by the tilted growth of grains on the side of the ingot.

The distribution of the resistivity equivalence lines in the vertical and cross sections are shown in Fig. 4. The shape of resistivity equivalence lines in the cross section was concave and that in vertical section was hemicyclic. The concentration of impurities in five different positions of the resistivity equivalence line of 3.3×10^{-3} Ω m in the cross section is shown in Table 2. The concentration of impurities in different positions of the resistivity equivalence line was nearly the same. The position having the same composition in directional growth ingot was on the same solid-liquid interface; therefore the resistivity equivalence lines in the vertical and cross sections were consistent with the solid-liquid interface during the solidification process. This indicated that the resistivity equivalence line in the cross section could be used to analyze the solid-liquid interface during the solidification process.

3.2 Effect of Impurity on the Distribution of Resistivity

The polarity measured in the bottom part of the vertical section was p-type, while that of the upper part was n-type. The transition position was around the breakdown area, corresponding to the changes of columnar grains to dendritic grains. Solidification fraction dependence of resistivity in the closed

Table 2 Primary concentration of impurities in five different positions of the same resistivity equivalence line (mass/$\times 10^{-6}$)

Position	Fe	Al	Ca	Ti	Cu	Ni	Mn	B	P
3	55.2	15.2	0	2.9	0.6	1.8	2.6	0.9	38.3
8	60.7	15.1	0	4.4	1.3	5.2	4.8	1.6	42.2
9	21.6	10.3	0	1.3	0.5	1.4	2.5	1.3	37.7
10	13.4	8.6	0	1.5	1.6	1.7	2.1	2.3	42.3
11	61.8	13.1	0	2.5	0.7	6.4	3.4	4.9	42.6

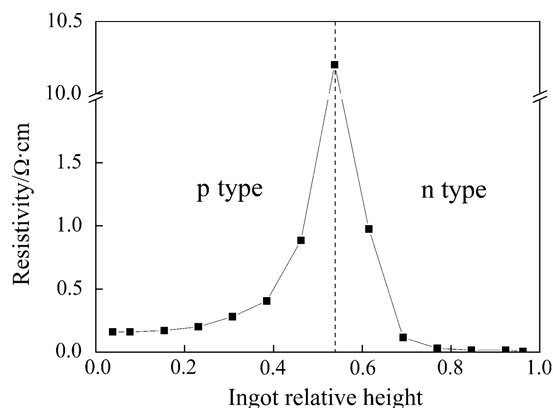

Fig. 5 Longitudinal distribution of resistivity in the center axial of the vertical section

white line area of Fig. 3(a) is shown in Fig. 5. The resistivity increased from 1.6×10^{-3} Ω m along the solidified height in the p-type area, and reached to the maximum value of 0.10 Ω m at the polarity transition position. With the increase of the solidified height, the polarity turned to n-type. In the n-type area, resistivity declined rapidly along the solidified height and approached zero at the top of the ingot because of the accumulation of the impurities.

Some studies (Ref 5, 6) indicated that the conductive type of silicon purified from metallurgical silicon was mainly determined by superposition effect of the concentration of P, B, and Al. Although the metal impurities could affect the resistivity of silicon, compared with P, B, and Al, their effects on the resistivity were small, and the residual contents of these elements were in the ppm range after directional solidification; therefore, their effects could be neglected alongside high concentrations of P, B, and Al, which existed. Based on the above discussion, only the concentration variations of P, B, and Al in the growth direction of the ingot were investigated in the current study. The effect of compounds on the carrier content was also neglected in this discussion because it was far less than that of elementary substances (i.e., the compounds of P, B, and Al existing in the ingot) formed when exceeding the solubility limit in silicon after the enrichment of the segregation. The maximum solid solubility of impurities in silicon is shown in Table 3 (Ref 10-13).

Figure 6 shows the solidified fraction dependence of the sum of the contents of Al and B and the content of P. The sum of the contents of Al and B increased slowly along the growth direction compared with the content of P. The sum of the contents of Al and B were higher than the content of P at the bottom part, while it was contrary at the top part.

Table 3 The highest solid solubility of impurities in silicon ($\times 10^{22}$)

Element	Fe	Ti	Cu	Ni	Mn	Al	B	P
Temperature, K	1479	1373	1075	1266	1415	1450	1424	1453
Solubility, atom/m^3	0.905	0.002	2.572	12.28	0.383	2147	24000	119856

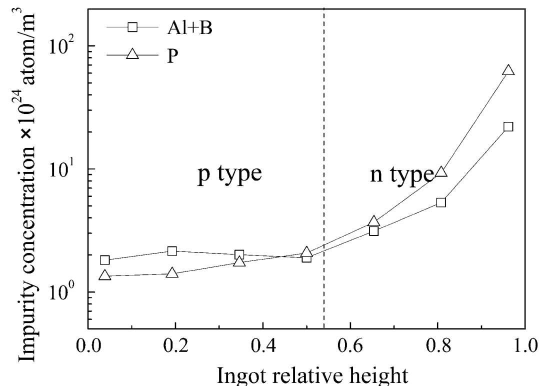

Fig. 6 Longitudinal content distribution of Al + B, and P in the vertical section

Although Al content increased exponentially because of its relative lower segregation coefficient of 2.8×10^{-3} (Ref 1), the extent of the increase of Al content was remarkably weakened for the Al content exceeding the maximum solid solubility was not considered. In the meantime, B content changed only slightly because of its large segregation coefficient (0.86). Therefore the sum of the contents of Al and B along the growth direction increased slowly. Because the saturated vapor pressure of P was much higher than that of liquid silicon, P was gradually enriched in the surface from the molten silicon during the melting process under a depressed Ar atmosphere. In addition, P had a relative small segregation coefficient 0.35 (Ref 1), and thus, the P content increased obviously along the growth direction and surpassed the sum of the contents of Al and B at the top of the ingot.

B and Al were acceptor impurities, generating hole carriers, while P was donor impurity, generating electronic carriers. At the bottom part, the sum of the Al and B contents was higher than that of P; therefore, the silicon was a p-type, and the hole carriers were the majority carriers. With the increase of P content in the growth direction, the hole carrier content decreased because of its combination with electron carriers generated by P. Thus, the resistivity in the p-type zone increased along the growth direction. At the point of polarity transition, the sum of the Al and B contents was nearly equal to that of P. All the hole carriers were nearly combined with the electron carriers generated by P. Because there were few carriers in silicon, the resistivity reached its maximum. At the top part, the situation was just the opposite. The P content was higher than the sum of the contents of Al and B; therefore, the silicon was n-type, with the electron carriers as the majority carriers. With further increase of P content in the growth direction, the amount of electron carriers gradually increased, and therefore, the resistivity in the n-type zone decreased along the growth direction. Results of the composition analysis showed that transition metals (e.g., Fe, Cu, and Ni) increased by two orders of magnitude during the directional solidification process, and exceeded their solubility limit at the top part of the silicon ingot; therefore, the metal impurities could not be ignored in these areas, and as a result, the resistivity at the top part of the silicon decreased remarkably and approached zero.

Although the resistivity was high in the p-n transition position, as shown in Fig. 5, with the relative height of the ingot relative height from the bottom being approximately 0.5, the compensation by impurities was obvious. The high concentration impurities introduced a deep level and became the combination center (Ref 1), and the structure of the material changed significantly, and therefore, it was not suitable for use in a solar cell.

4. Conclusions

Based on the above discussion, the shape of the equivalence line of the resistivity in the vertical and cross sections was considered to be determined by the solid-liquid interface. It could be used to analyze the variation of the solid-liquid interface. Along the solidification height of the silicon ingot, the conductive type changed from p-type at the lower part of the silicon ingot to n-type at the upper part of the silicon ingot. The resistivity in the vertical section of the silicon ingot initially increased along the height of the solidified part, and reached its the maximum at the polarity transition position, and then decreased rapidly along the height of the solidified part and approached zero on the top of the ingot because of the accumulation of impurities. The variation of resistivity in the vertical section of the ingot was proven to be deeply relevant to the distribution of Al, B, and P in the growth direction of solidification.

Acknowledgments

This program is financially supported by the Key Technologies R&D Program of Liaoning, China (2006222007), and the Dalian Science and Technology Program (20090231).

References

1. K. Morita and T. Miki, Thermodynamics of Solar-Grade-Silicon Refining, *Intermetallics*, 2003, **11**(11–12), p 1111–1117
2. A.A. Istratov, T. Buonassisi, M.D. Pickett, M. Heuer, and E.R. Weber, Control of Metal Impurities in "Dirty" Multicrystalline Silicon for Solar Cells, *Mater. Sci. Eng. B*, 2006, **134**(2–3), p 282–286
3. C. Alemany, C. Trassy, B. Pateyron, K.-I. Li, and Y. Delannoy, Refining of Metallurgical-Grade Silicon by Inductive Plasma, *Sol. Energy Mater. Sol. Cells*, 2002, **72**(1–4), p 41–48
4. A.F.B. Braga, S.P. Moreira, P.R. Zampieri, J.M.G. Bacchin, and P.R. Mei, New Processes for the Production of Solar Grade Polycrystalline Silicon: A Review, *Sol. Energy Mater. Sol. Cells*, 2008, **92**(4), p 418–424
5. J. Degoulange, I. Périchaud, C. Trassy, and S. Martinuzzi, Multicrystalline Silicon Wafers Prepared from Upgraded Metallurgical Feedstock, *Sol. Energy Mater. Sol. Cells*, 2008, **92**(10), p 1269–1273
6. S. Binetti, J. Libal, M. Acciarri, M. Di Sabatino, H. Nordmark, E.J. Øvrelid, J.C. Walmsley, and R. Holmestad, Study of Defects and Impurities in Multicrystalline Silicon Grown from Metallurgical Silicon Feedstock, *Mater. Sci. Eng. B*, 2009, **159**(15), p 274–277

7. B.N. Mukashev, Kh.A. Abdullin, M.F. Tamendarov, T.S. Turmagambetov, B.A. Beketov, M.R. Page, and D.M. Kline, A Metallurgical Route to Produce Upgraded Silicon and Monosilane, *Sol. Energy Mater. Sol. Cells*, 2009, **93**(10), p 1785–1791
8. E. Enebakk, K. Friestad, R. Tronstad, C. Zahedi, and C. Dethloff, Silicon Feedstock for Solar Cells, U.S. Patent 20070128099, 7 Jun 2007
9. M. Dhamrin, T. Saitoh, I. Yamaga, and K. Kamisako, Compensation Effect of Donor and Acceptor Impurities Co-Doping on the Electrical Properties of Directionally Solidified Multicrystalline Silicon Ingots, *J. Cryst. Growth*, 2009, **311**(3), p 773–775
10. E.R. Weber, Transition Metals in silicon, *Appl. Phys. A*, 1983, **30**(1), p 1–22
11. T. Yoshikawa and K. Morita, Solid Solubilities and Thermodynamic Properties of Aluminum in Solid Silicon, *J. Electrochem. Soc.*, 2003, **150**(8), p 465–468
12. G.L. Vick and K.M. Whittle, Solid Solubility and Diffusion Coefficients of Boron in Silicon, *J. Electrochem. Soc.*, 1969, **116**(8), p 1142–1144
13. R.W. Olesinski, N. Kanani, and G.J. Abbaschian, The P-Si(Phosphorous-Silicon)System, *Bull. Alloys Phase Equilib.*, 1985, **6**(2), p 130–133